

Investigating the Effect of Changing Plasma Electrolytic Oxidation on the Scratch Degradation of Ti-6Al-4V

M. R. Tavighi^{1,*}, A. Rabieifar¹, O. Ashkani², A. Asaadi-Zahraei³

¹Advanced Materials Engineering Research Center, Karaj Branch, Islamic Azad University, Karaj, Iran.

²Faculty of Technology and Engineering, Science and Research Branch, Islamic Azad University, Tehran, Iran.

³Faculty of Materials Science and Engineering Khajeh Nasir Toosi University, Tehran, Iran

Received: 02 February 2024 - Accepted: 10 June 2024

Abstract

In this research, plasma electrolytic oxidation (PEO) was prepared at duty voltage of 350 and 450 V and processing time of 5 and 10 minutes on Ti-6Al-4V alloy in Na₂SiO₃ + KOH electrolyte. Then, the adhesion strength and microstructural degradation of the coating surface were investigated through a constant load scratch test, field-emission scanning electron microscope (FE-SEM), and X-ray diffraction (XRD), respectively. The results showed that while increasing the processing time and duty voltage, the density of porosity and the amount of rutile on the coating surface increased. Meanwhile, microstructure degradations like delamination, gross spallation, and buckling spallation decreased due to increased adhesion strength. This resulted from an increase in voltage and processing time.

Keywords: Plasma Electrolytic Oxidation (PEO), Ti6Al4V Alloy, Scratch Test, Degradation Mechanisms.

1. Introduction

Plasma electrolysis oxidation (PEO) or micro-arc oxidation (MAO) is one method of producing surface porosity in light metals such as aluminum, magnesium, titanium, and their alloys before applying polymer coatings [1]. This method involves placing the workpiece in an aqueous alkaline electrolyte, and dissolving the salts (mostly sodium silicate and potassium hydroxide) in it [2]. As a result of the high potential difference in this process, the produced oxide layer suddenly breaks and turns into a plasma. High-speed oxidation takes place on the surface. This process results in a tough ceramic surface on the substrate [3].

Plasma oxidation electrolysis involves maintaining a constant current and increasing the applied voltage. As a result, the insulated oxide layer breaks, its growth on the surface is halted, and tiny sparks are generated. Sparking is one of the distinctive characteristics of this process and what distinguishes it from other coating methods. It leads to the absorption of alloy elements and the formation of the final coating [4]. There is a very high electrical discharge in the electrolyte bath. Electrical discharge occupies an essential part of the process, and this can form a porous structure and improve adhesion strength [5]. The PEO coating microstructure is often jagged and wavy. Its thickness is proportional to the method variables, usually in the range of 5-200 μm [6]. In general, all PEO coatings are composed of two layers with different morphologies: the inner protective layer with a thickness of about a few nanometers to 2 μm

and the outer layer, which forms during the electrical discharge process and includes voids and porosity on the surface [7]. Oxidation electrolysis plasma coating has many industrial applications due to its high hardness, wear resistance, and corrosion resistance [8]. Choosing the type of electrolyte, potential difference, working period, current intensity, oxidation micro-arc time, and prior treatments and post-treatment affects the morphology and structure of the coating [9-11].

Pure titanium is widely used in medical applications and for medical implants [12]. Nevertheless, the formability and wear resistance of pure titanium is poor, which can increase the risk of implant failure [13-15]. Therefore, adding alloying elements to titanium improves its alloy properties [16]. Recently, beta titanium alloys, including the non-toxic alloy elements of Nb, Zr, and Ta, with high superelasticity and suitable biocompatibility, have been developed [17-20].

Yao et al. [21] studied the PEO coating method on Ti-6Al-4V alloy. They announced that the coatings produced on the titanium samples had a surface roughness of about 8.11-11.6 μm and were white in appearance. They found that increasing the current density causes an increase in the thickness and roughness of the coatings. In contrast, increasing frequency causes a decrease in thickness and roughness. However, changing the current density and working frequency does not affect the coating phase composition. Zhou et al. [22] studied the high-temperature oxidation resistance of PEO coatings on Ti-6Al-4V alloys at temperatures of 700°C and 1000°C with electrolyte solutions containing different concentrations of Na₂SiO₃, 4 g/l Na₂CO₃ and 0.5 g/l NaOH.

*Corresponding author

Email address: mr.tavighi@kiaou.ac.ir

Table 1. Chemical composition (wt.%) of Ti6Al4V alloy.

Al	V	C	N	O	Fe	H	Ti
6.000	4.200	0.030	0.010	0.150	0.100	0.003	Bal.

They reported that the ceramic coating consisted of TiO₂, rutile, and anatase phases. Increasing the concentration of Na₂SiO₃ led to a gradual decrease in TiO₂ and an increase in the coating thickness. Hao et al. [23] and Tang et al. [24] investigated the effects of the PEO process on high-temperature oxidation-resistant coatings of TiAl alloys at temperatures of 850°C and 1000°C. They found that during the PEO process, TiAl alloys' high-temperature oxidation resistance improved. Chan et al. [24], while investigating the corrosion and wear resistance of beta titanium alloy in the N₂ atmosphere, found that the thickness and density of the coating increased with the increase of the processing time in the electrolyte solution. Fan et al. [25] studied the effect of oxidation voltage on the morphology of TiO₂-containing apatite coating. The MAO process was done in 2 minutes in H₂SO₄ electrolyte at 90 to 100 V and then the samples were immersed in a solution containing Apatite for seven days. They found that by increasing the voltage from 90 to 100 V, the thickness of the TiO₂ layer, the capacity to form apatite, and the average diameter of the voids increased. Ping et al. [26] produced titanium with different coatings under different current intensities by the MAO method in NaAlO₂ electrolyte on titanium alloy. The results showed that the coating phases produced were Anatase and Rutile. Also, with the increase in MAO current intensity, the amount of the Rutile phase and the size of the voids increased. In contrast, the surface roughness and Anatase phase decreased.

2. Materials and Methods

In this research, Ti-6Al-4V alloys were produced in a vacuum electric arc remelting furnace. They were used with a size of 50 mm × 25 mm × 2 mm with Table 1. chemical composition as substrate for MAO coating process.

Prior to MAO coating, the samples were mechanically polished with abrasive paper up to a grit of 2000. A stream of hot air at 60°C was used to dry them after they had been degreased with acetone and rinsed with deionized water.

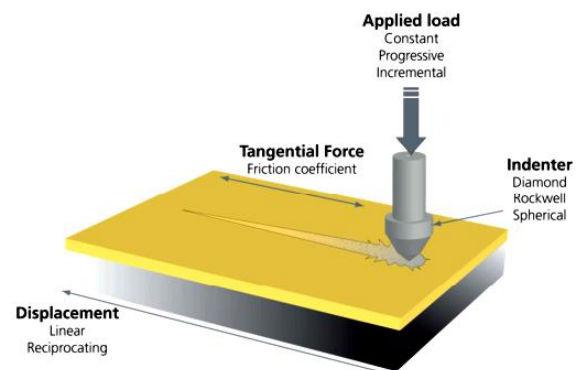
The treatment device for micro-arc oxidation process consists of a power generator, a one L glass container was used as an electrolytic cell, and as a stirring and cooling system. For the MAO coating experiments, a pulse power generator (MIRDC) with two working voltages, two processing times (according to Table 2.), a current up to 10 A, a duty cycle of 5%-95%, and a frequency range of 500-5000 Hz was used. The stainless steel plate and the Mg alloy substrate were used as the cathode and

anode, respectively. The MAO treatments were conducted in the electrolyte containing 150 g/L Na₂SiO₃ and 3 g/L KOH. During the oxidation process, the solution was stirred at a rate of 300 rpm and cooled to a temperature of 25°C. In this situation, sparking during coating was performed at low intensity. MAO treatments were performed using pulsed bipolar current mode. While the process was in progress, the positive duty cycle was set at 40% and the magnitude of the negative current density was equal to that of the positive one. The surface adhesion strength of the applied coatings was checked by a scratch test. The standard diamond stylus used for scratch testing had Rockwell C geometry with a 120° cone and a spherical tip of 200 μm radius. The loading rate was 100 N/min and the indenter reciprocating speed was 10 mm/min (Fig. 1).

Microstructural studies were conducted with a MIRA3-Tescan field-emission scanning electron microscope (FESEM). X-ray diffraction was performed using a Philips-PW1730 diffractometer with monochromatic radiation of Cu Kα (λ = 1.54060 Å). The voltage and current were 40 kV and 30 mA, respectively. X-pert High Score software was used for phase identification in XRD.

Table 2. Samples and variables of the PEO process

Sample No.	Processing time (min)	Voltage (V)
Ti1	5	350
Ti2	10	350
Ti3	5	450
Ti4	10	450

**Fig. 1. Schematic of the scratch test on the surface of the coated samples.**

3. Results and Discussion

The cross-sectional morphologies of PEO coatings for Ti1, Ti2, Ti3, and Ti4 samples are shown in Fig. 2., respectively.

The PEO coating consisted of two porous and dense layers. In the early stages of the deposition process, an amorphous porous layer with low hardness was formed on the substrate. This layer had little adhesion due to rapid electrolyte cooling. With the increase in oxidation time, the dense ceramic crystal layer also formed and grew towards the substrate [27].

The thickness of the PEO coating increases with increasing processing time and voltage, as seen in Fig. 2. Furthermore, the size of coating porosities increases with processing times and voltages. PEO coatings are very porous and rough due to micro discharges during the PEO process.

The outer layer of PEO coatings is amorphous owing to the rapid cooling rate of the electrolyte, and its adhesion to the substrate surface was weak. In addition, the interior layer of PEO coatings is crystalline and dense due to high temperature and high pressure. Therefore, the inner layer of the coatings is denser and tougher than the outer layer of the coatings. The thickness of the dense layer close to the substrate increases with processing time as well as duty voltage.

The FE-SEM image of the coating surface of Ti1 and Ti2 samples is shown in Fig. 3. The sample's coating surfaces had spherical pores.

By comparing the observations of the coating surface of Ti1 and Ti2 samples, it is clear that increasing the sparking duration or increasing the coating applying duration will lead to an increase in the porosity of the coating surface [28]. Porosities formation indicates the inhomogeneous growth of PEO coating layers. Moreover, apparent protrusions in the vicinity of large porosities indicate re-deposition of melted coating materials after the localized dielectric breakdown of the layer [3].

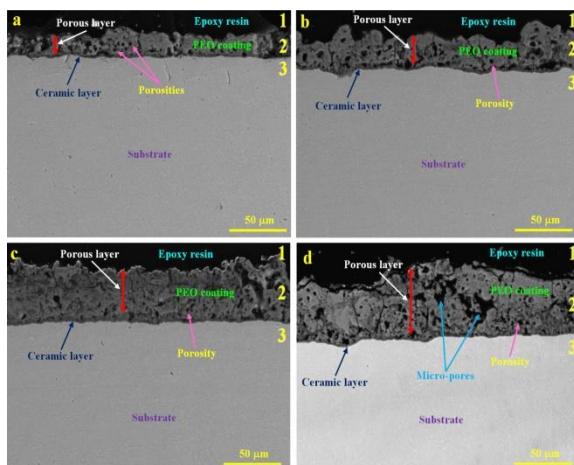


Fig. 2. The cross-sectional SEM morphologies of the PEO coatings for: (a) Ti1, (b) Ti2, (c) Ti3 and (d) Ti4 samples.

The X-ray diffraction pattern (XRD) of Ti1 and Ti2 samples is shown in Fig. 4. The coating created in

both samples was relatively crystalline and mainly composed of Anatase and Rutile phases.

The beta titanium phase in the diffraction pattern was attributed to the substrate and had a relatively high intensity. The TiO_2 layer was formed due to titanium oxidation during the PEO process at the oxide/titanium coating interface [29]. For this reason, the titanium concentration was higher in the early stages of the oxidation process.

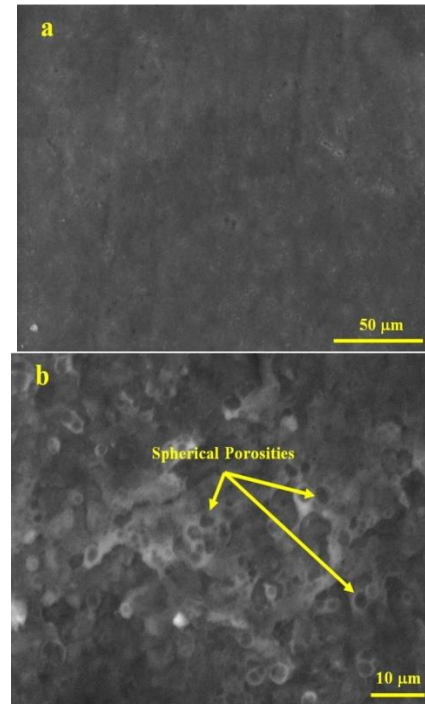


Fig. 3. FE-SEM image of the coating surface in: a: Ti1, b: Ti2 samples.

The FE-SEM image of the coating surface of the Ti3 and Ti4 samples is shown in Fig. 5. The applied voltage of the PEO process in these samples has increased compared to the two Ti1 and Ti2 samples. As can be seen, increasing the voltage created more porosity and micro-pores in the formed layer.

Also, extending the processing time in the electrolyte solution (comparing Ti3 and Ti4 samples) due to the longer ignition time led to an increase in the coating thickness as well as an increase in its porosity [30, 31]. The porosities present were spherical, and their amount in the Ti4 sample was more than in other samples.

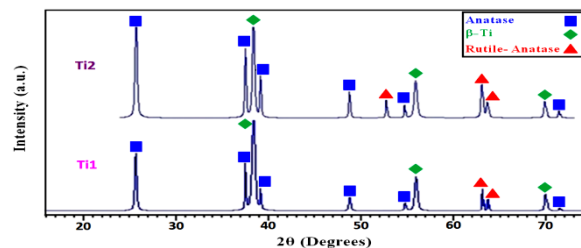


Fig. 4. XRD results of Ti1 and Ti2 samples.

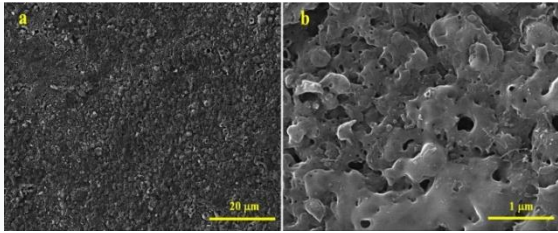


Fig. 5. FE-SEM image of the coating surface in: a: Ti3, b: Ti4 samples.

The X-ray diffraction (XRD) pattern of Ti3 and Ti4 samples is shown in Fig. 6. As can be seen, the frequency and intensity of rutile (TiO_2) peaks increased with increasing voltage and processing time (compare Fig. 4. and Fig. 6.). FE-SEM images of Ti1, Ti2, Ti3, and Ti4 samples after the scratch test are shown in Fig. 7. to Fig. 10., respectively.

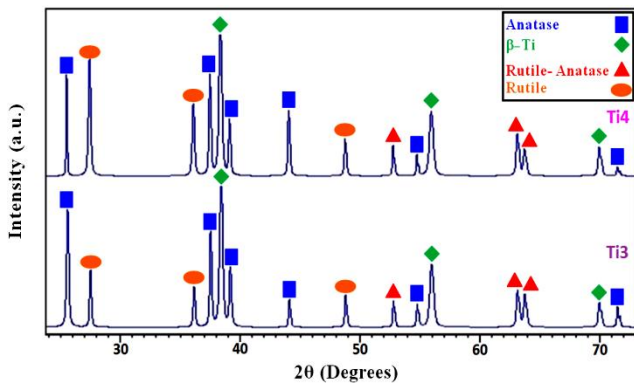


Fig. 6. XRD results of Ti3 and Ti4 samples.

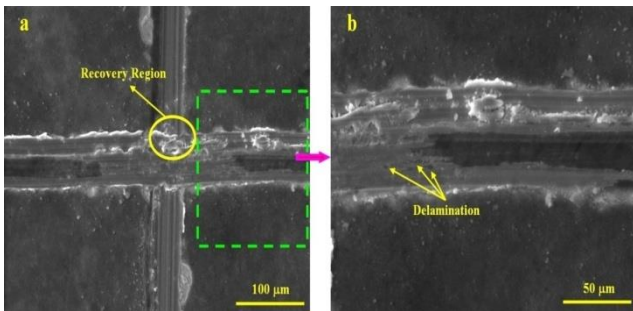


Fig. 7. a: FESEM image of Ti1 coating surface after the scratch test, b: the area marked in fig. a.

As can be seen, the Ti1 sample had recovery areas. Due to the movement of the indenter, some areas inside the grooves created in the coating suffered delamination and spallation (Fig. 7.).

In a part of the Ti2 sample surface coating, dimples were observed inside and outside the scratched area (Fig. 8.b).

Also, more chips were observed on the surface of this sample than on other samples. Gross spallation is a term used to describe a large amount of pull-off of the Ti3 surface coating. Pull-off occurrence was caused by the low adhesive strength of the coating and occurred in areas of considerable extent.

Also, buckling spallation occurred in some areas, during which irregular holes were formed in the scratched path [32].

However, in the scratched path of the Ti4 coating surface, there was no sign of cracks and roughness. This issue was caused by the high adhesive strength of the coating of this sample compared to samples Ti1 and Ti2 due to the increasing amount of Rutile on the surface of Ti4 sample [33].

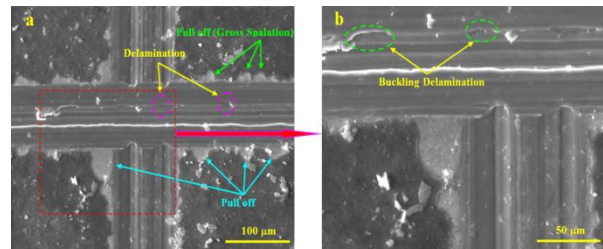


Fig. 8. a: FESEM image of Ti2 coating surface after the scratch test, b: the area marked in fig. a.

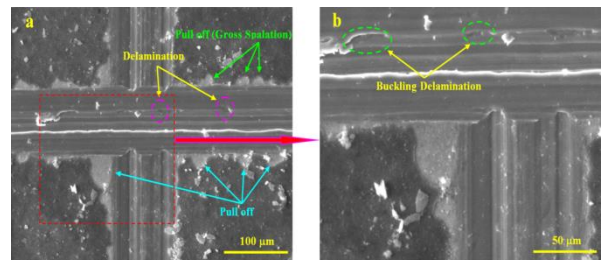


Fig. 9. a: FESEM image of Ti3 coating surface after the scratch test, b: the area marked in fig. a.

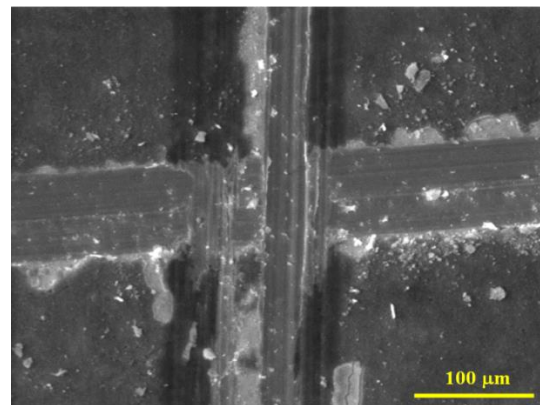


Fig. 10. FE-SEM image of Ti4 coating surface after scratch test.

4. Conclusion

In the present research, the microstructural changes and degradation mechanisms of the Ti-6Al-4V alloy due to scratch tests after PEO at different duty voltages and processing times were investigated. The results were as below:

1. The thickness of the PEO coating and the size of coating porosities increased with increasing processing time and duty voltage.

2. By increasing the duty voltage, the density of created porosity and micro-pores in the formed layer was increased.
3. By increasing the duty voltage and processing time, the density of Rutile on the surface of the PEO coating increased.
4. By increasing the duty voltage and processing time, the occurrence of delamination, gross spallation, and buckling spallation was reduced.

References

- [1] Sikdar S, Menezes PV, Maccione R, Jacob T, Menezes PL. Plasma electrolytic oxidation (PEO) process—processing, Charact. appl. nanomater. 2021, 22;11(6):1375.
- [2] Simchen F, Sieber M, Kopp A, Lampke T. Introduction to plasma electrolytic oxidation—An overview of the process and applications. Coatings. 2020, 30;10(7):628.
- [3] Lu X, Chen Y, Blawert C, Li Y, Zhang T, Wang F, Kainer KU, Zheludkevich M. Influence of SiO₂ particles on the corrosion and wear resistance of plasma electrolytic oxidation-coated AM50 Mg alloy. Coatings. 2018, 29;8(9):306.
- [4] Wang JH, Wang J, Lu Y, Du MH, Han FZ. Effects of single pulse energy on the properties of ceramic coating prepared by micro-arc oxidation on Ti alloy. Appl. Surf. Sci., 2015, 1;324:405-13.
- [5] Dong H. Tribological properties of titanium-based alloys. Surf Eng Light Alloys., 2010, 1 (58-80). Woodhead Publishing.
- [6] Darband GB, Aliofkhaezai M, Hamghalam P, Valizade N. Plasma electrolytic oxidation of magnesium and its alloys: Mechanism, properties and applications. J. Magnes Alloys., 2017, 1;5(1):74-132.
- [7] Clyne TW, Troughton SC. A review of recent work on discharge characteristics during plasma electrolytic oxidation of various metals. Int. Mater. Rev. 2019;64(3):127-62.
- [8] Srinivasan PB, Blawert C, Dietzel W. Effect of plasma electrolytic oxidation treatment on the corrosion and stress corrosion cracking behaviour of AM50 magnesium alloy. Mater. Sci. Eng.: A. 2008, 25;494(1-2):401-6.
- [9] Songur F, Dikici B, Niinomi M, Arslan E. The plasma electrolytic oxidation (PEO) coatings to enhance in-vitro corrosion resistance of Ti–29Nb–13Ta–4.6 Zr alloys: The combined effect of duty cycle and the deposition frequency. Surf. Coat. Technol. 2019, 25;374:345-54.
- [10] Vakili-Azghandi M, Fattah-Alhosseini A. Effects of duty cycle, current frequency, and current density on corrosion behavior of the plasma electrolytic oxidation coatings on 6061 Al alloy in artificial seawater. Metall. Trans.Mater., A. 2017;48:4681-92.
- [11] Fattah-Alhosseini A, Keshavarz MK, Molaei M, Gashti SO. Plasma electrolytic oxidation (PEO) process on commercially pure Ti surface: effects of electrolyte on the microstructure and corrosion behavior of coatings. Metall. Trans. Mater. A. 2018;49:4966-79.
- [12] Romeo E, Lops D, Margutti E, Ghisolfi M, Chiapasco M, Vogel G. Long-term survival and success of oral implants in the treatment of full and partial arches: a 7-year prospective study with the ITI dental implant system. Int. J. Oral Maxillofac Implants., 2004, 1;19(2).
- [13] McCracken M. Dental implant materials: commercially pure titanium and titanium alloys. J.Prostodont. 1999;8(1):40-3.
- [14] Zinsli B, Sägger T, Mericske E, Mericske-Stern R. Clinical evaluation of small-diameter ITI implants: a prospective study. Int. J. Oral Maxillofac Implants.2004, 1;19(1).
- [15] Chrcanovic BR, Kisch J, Albrektsson T, Wennerberg A. Factors influencing the fracture of dental implants. Clin. Implant Dent.Relat. Res. 2018;20(1):58-67.
- [16] Cordeiro JM, Barão VA. Is there scientific evidence favoring the substitution of commercially pure titanium with titanium alloys for the manufacture of dental implants. Mater. Sci. Eng.: C. 2017, 1;71:1201-15.
- [17] Elias LM, Schneider SG, Schneider S, Silva HM, Malvisi F. Microstructural and mechanical characterization of biomedical Ti–Nb–Zr(–Ta)alloys. Mater. Sci. Eng. A. 2006 25;432(1-2):108-12.
- [18] Cordeiro JM, Beline T, Ribeiro AL, Rangel EC, da Cruz NC, Landers R, Faverani LP, Vaz LG, Fais LM, Vicente FB, Grandini CR. Development of binary and ternary titanium alloys for dental implants. Dent. Mater. 2017, 1;33(11):1244-57.
- [19] Guo Y, Chen D, Lu W, Jia Y, Wang L, Zhang X. Corrosion resistance and in vitro response of a novel Ti35Nb2Ta3Zr alloy with a low Young's modulus. Biomed. Mater. 2013, 3;8(5):055004.
- [20] Stenlund P, Omar O, Brohede U, Norgren S, Norlindh B, Johansson A, Lausmaa J, Thomsen P, Palmquist A. Bone response to a novel Ti–Ta–Nb–Zr alloy. Acta Biomater. 2015, 1;20:165-75.
- [21] Yao Z, Su P, Shen Q, Ju P, Wu C, Zhai Y, Jiang Z. Preparation of thermal control coatings on Ti alloy by plasma electrolytic oxidation in K₂ZrF₆ solution. Surf. Coat. Technol. 2015, 15;269:273-8.
- [22] Zhou H, Liu Z, Li Z, Du J. Microarc oxidation coating and high-temperature oxidation resistant property on Ti alloy. Rare Metal Mater. Eng. 2005;34(11):1835-8.
- [23] Hao J, Jie W, Chen H, Ye Y. The Effect of SiO₂ on Micro-Arc Oxidation Ceramic Layer of TiAl Alloy. Rare Metal Mater. Eng., 2005;34(9):1455-9.
- [24] Z.L. Tang, F.H. Wang and W.T. Wu, Effect of micro-arc oxidation treatment on oxidation

resistance of TiAl alloy, *Chin. J. Non-ferrous Met.*, Vol. 9, 1999, p 63–8.

[25] Fan XP. Effects of process parameters on microarc oxidation film layers of porous titanium. *Appl. Ecol. Environ. Sci.* 2019, 1;17(4).

[26] Ping W, Ting W, Hao P, Yang GX. Effect of NaAlO₂ concentrations on the properties of microarc oxidation coatings on pure titanium. *Mater. Letters*. 2016, 1;170:171-4.

[27] Wang S, Liu X, Yin X, Du N. Influence of electrolyte components on the microstructure and growth mechanism of plasma electrolytic oxidation coatings on 1060 aluminum alloy., *Surf. Coat. Technol.* 2020, 15;381:125214.

[28] Yao Z, Shen Q, Niu A, Hu B, Jiang Z. Preparation of high emissivity and low absorbance thermal control coatings on Ti alloys by plasma electrolytic oxidation. *Surf. Coat. Technol.*, 2014, 15;242:146-51.

[29] Xue W, Wang C, Chen R, Deng Z. Structure and properties characterization of ceramic coatings produced on Ti–6Al–4V alloy by microarc oxidation in aluminate solution., *ACS Mater. Lett.* 2002, 1;52(6):435-41.

[30] Shokouhfar M, Dehghanian C, Montazeri M, Baradaran AJ. Preparation of ceramic coating on Ti substrate by plasma electrolytic oxidation in different electrolytes and evaluation of its corrosion resistance: Part II. *Appl. Surf. Sci.*, 2012, 15;258(7):2416-23.

[31] Durdu S, Usta M. The tribological properties of bioceramic coatings produced on Ti6Al4V alloy by plasma electrolytic oxidation. *Ceram. Int.*, 2014, 1;40(2):3627-35.

[32] Wei D, Zhou Y, Guo H. Characterization and properties of microarc oxidized coatings containing Si, Ca and Na on titanium. *Ceram. Int.*, 2011 1;37(6):1761-8.

[33] Sharifi H, Aliofkhaezrai M, Darband GB, Shrestha S. A review on adhesion strength of peo coatings by scratch test method. *Surf. Rev. Lett.* 2018 25;25(03):1830004.